MECHANICAL ENGINEERING

Use of the VAP function in the design of cam-follower mechanisms

INGENIERIA MECÁNICA

Uso de la función VAP en el diseño de mecanismos leva seguidor

Héctor F. Quintero*§, Libardo V. Vanegas*

**Mechanical Engineering Faculty, Universidad Tecnológica de Pereira. Pereira, Colombia.*
§hquinte@utp.edu.co, lvanegas@utp.edu.co

(Recibido: Diciembre 09 de 2015 – Aceptado: Abril 11 de 2016)

Abstract

A new mathematical periodic function, called VAP function, is proposed for the design of cam-follower mechanisms. With the VAP function, a given variable increases and decreases almost linearly from its minimum and maximum values, respectively, while the function and its derivate are smooth. As a case study, the design of a disc cam with a translating roller follower is considered, using four displacement laws: one based on a 4-5-6-7 polynomial displacement function, one based on a harmonic function, and two based on the VAP function. A comparative dynamic and kinematic analysis is shown. It is concluded that the cam-follower mechanism designed with the VAP function has smaller input torques, as well as lower pressure angles, than the one designed with harmonic function and that the one with 4-5-6-7 polynomial function.

Keywords: *Cam-follower mechanisms, dynamic analysis, kinematic analysis, VAP function.*

Resumen

Se propone una nueva función matemática periódica, llamada función VAP, para el diseño de mecanismos leva seguidor. Con la función VAP, una variable aumenta y decrece casi linealmente desde sus valores mínimo y máximo, respectivamente, pero la función y su derivada son suaves. Se considera el diseño de una leva de disco con un seguidor de rodillo radial, utilizando cuatro leyes de desplazamiento: una basada en la función polinomial 4-5-6-7, una basada en una función armónica y dos basadas en la función VAP. Se realiza un análisis dinámico y cinemático. Se concluye que el mecanismo leva seguidor diseñado con la función VAP tiene menores pares motor, así como menores ángulos de presión, que los obtenidos con el diseñado con la función armónica y con la función polinomial 4-5-6-7.

Palabras clave: *Análisis cinemático, análisis dinámico, función VAP, mecanismo leva seguidor.*

1. Introduction

Cam–follower mechanisms are used extensively in modern machines, due to their various attractive features, such as design simplicity, low manufacturing costs, and versatility (Gatti & Mundo, 2010). Consequently, many researchers have proposed new designs or features related to cam-follower mechanisms. For example, some works have studied cam applications; an inverter cam mechanism for input torque balancing a high-speed, industrial cam-follower mechanism is designed and optimized (Demeulenaere & De Schutter, 2004). A cam-based lower-limb prosthesis is designed to achieve a nonlinear response of the powered ankle prosthesis, as well as to reduce the required actuator torque (Realmuto et al., 2015). According to the results, the introduction of the cam-based element may reduce the maximum torque required by about 74%. Lower and upper legs of a single-degree-of-freedom robotic leg are controlled by two cams mounted on one shaft (Peters & Chen, 2014). An optimization process is developed based on the kinematic equations. The optimization includes an objective function, namely minimization of the difference between the position of the foot and its desired position, as well as some design constraints.

There are also works that study the characteristics of the motion law used in the cam-follower mechanisms. For example, a closed-form modified trapezoidal function with adjustable positive and negative acceleration is proposed in order to design cam motion function (Flockers, 2012); the cam profile designed is adequate for applications in which there are various dwells or for high speed cams in which the follower acceleration has to be controlled. In (Flores, 2013) a computational methodology for the optimized design of disc-cam mechanisms with eccentric translating roller followers is presented; the objective function takes into account: the cam base circle radius, the roller radius, and the follower offset.

With respect to dynamic studies, for example, (Jiang & Iwai, 2009) presents a method for designing dynamically-compensated (tuned) cams; the improved method minimizes or limits vibrations in high-speed cam-follower mechanisms. In (Catalá et al., 2013) the effect of the amount of interference fit planned of a conjugated cam system on the dynamic response is evaluated; using a Monte Carlo study, it analyzes how the amount of external offset added to the profiles of the cams, the quality of the manufactured cam profiles, manufacturing errors, and some inherent errors, such as clearances, affect the contact forces, the expected fatigue life, the contact pressures, and lubricant conditions.

As some cam-follower devices, such as automotive engine valve trains, run at very high speeds, the profiles of the cams have to be refined with precision in order to ensure the kinematic and dynamic characteristics (Kim, 1990). In some applications, it is necessary to control the displacement curve, the velocity curve, the acceleration curve, and even the jerk curve. The functions of standard motions include harmonic, cycloid, modified harmonic, trapezoidal, modified trapezoidal, and polynomial. In (Flocker, 2012b) an asymmetric acceleration-derived cam motion program is presented; the designed program is intended for a single-dwell cam-follower mechanism in which there is a clearance between the cam and follower during dwell; the aim of the program is to control the ratio of the positive and negative accelerations. In (Hsein, 2010), a methodology for designing and analyzing cams with three circular-arc profiles is presented. In this method a generic geometric model of the cam profile is defined, and the corresponding equations of the circular arcs are derived using a homogeneous coordinate transformation approach.

Recently, new functions are used to design the follower motion; for example, spline (Nguyen & Kim, 2007; Mermelstein & Acar, 2003), B-spline (Jiang & Iwai, 2009), and Bézier curves (Hidalgo et al., 2014) have been successfully applied in cam

design. In (Hseih, 2010) an improved approach for designing flexible cam profiles is proposed; the method makes use of smoothing spline curves and aims at controlling kinematic properties: displacement, velocity, and acceleration, as well as dynamic characteristics. Spline methods are flexible enough to permit motion programs to be refined or optimized while still satisfying motion constraints (Nguyen & Kim, 2007). There are other applications in which it is also necessary to smooth a function; for example, in (Quintero et al., 2007) Bézier and B-spline nonparametric curves are used for defining the relationship between the angular coordinates of N-lobe noncircular gears.

In this article, we utilize a new mathematical smooth periodic function, named VAP, in the design of a follower motion law. The VAP function may be tailored to produce a small, almost minimum difference between the maximum and minimum values of its derivative. Originally, this mathematical function was developed to attain small driven shaft accelerations in a noncircular gear pair system (Vanegas et al., 2006). A constant velocity and a harmonic function are also used to define the follower motion law. A dynamic analysis is formulated in order to calculate the input torque and the follower-cam contact forces. A comparison of pressure angles, contact forces, and input torques is shown in this work for the cam-follower mechanisms that deliver the displacement laws studied.

2. The VAP mathematical function

The idea from which the function has been devised is illustrated by means of Fig. 1. The periodic function of interest, $y(x)$, varies between certain minimum, y_{min}, and maximum, y_{max}, values. This function may be characterized by the mean, y_m, and alternating, y_a, parameters, as well as the period τ. In order to achieve the minimum value of the maximum derivative, y'_{max}, and the maximum value of the minimum derivate, y'_{min}, for a given set of values y_m, y_a, and τ, the function has to be a triangle wave. However, this curve is not smooth, and its derivative has sudden changes (Vanegas et al., 2006).

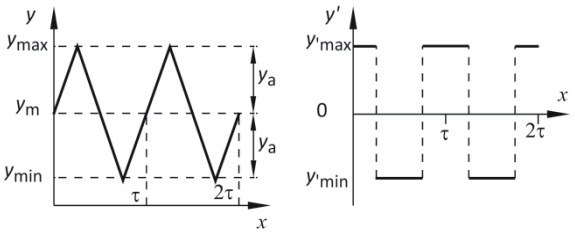

Figure 1. *A triangular function and its derivate. a) Triangular function, b) square function.*

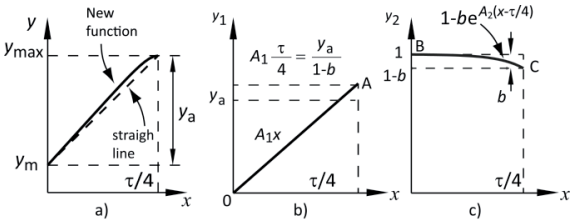

Figure 2. *Auxiliary functions for deriving the VAP function. (a) Fundamental VAP function; (b) auxiliary linear function $A_1 x$; (c) auxiliary exponential function.*

In order to obtain smooth curves for $y(x)$ and $y'(x)$, a mathematical function has been developed (Vanegas et al., 2006). The minimum absolute values of y'_{max} and y'_{min} are achieved when y varies linearly (see Fig. 1 and dashed line in Fig. 2(a)). The VAP function is conceived so that its slope is approximately constant and slightly greater than that of the straight dashed line, excepting that when x is close to τ /4, the slope quickly becomes zero. It is necessary that the slope is zero at $x = \tau/4$ so that both y and y' are smooth. The developed function is (Vanegas et al., 2006):

$$y(x) = y_m + A_1 x\left(1 - b\,e^{A_2\left(x-\frac{\tau}{4}\right)}\right) \qquad (1)$$

The function is the sum of the parameter y_m and the product of the linear function $A_1 x$ (line OA in Fig. 2(b)) and the exponential function within brackets; this can be controlled in order that it is virtually constant, excepting when x is close to τ /4 (curve BC in Fig. 2(c)). A curve smoothing equation has a smoothness term (Chan et al., 2005). In eq. (1), the "smoothness parameter" b, which belongs to the range (0,1), defines the exact shape of the curve; when it is close to zero,

the function is similar to a triangle wave and, consequently, is less smooth.

The parameters A_1 and A_2 are obtained from boundary conditions at $x = 0.25\,\tau$ (Vanegas et al., 2006):

$$y(0.25x) = y_{\mathrm{m}} + y_a \text{ and } \frac{\mathrm{d}y}{\mathrm{d}x}(0.25x) = 0 \qquad (2)$$

Therefore, eq. (1) yields

$$y(x) = y_{\mathrm{m}} + \frac{4y_{\mathrm{a}}}{1-b}\frac{x}{\tau}\left(1 - b\,\mathrm{e}^{\frac{1-b}{b}\left(4\frac{x}{\tau}-1\right)}\right) \qquad (3)$$

Eq. (3) is applicable only for $0 \le x \le \tau/4$. The VAP function, which is valid for $0 \le x < \tau$, is given by (Vanegas et al., 2006)

$$y(x) = y_{\mathrm{m}} + \frac{2y_{\mathrm{a}}}{1-b}h_1(x)\left(1 - b\,\mathrm{e}^{\frac{1-b}{b}(2h_2(x)-1)}\right) \qquad (4)$$

where

$$h_1(x) = \frac{1}{\pi}\arcsin\left(\sin\left(\frac{2\pi x}{\tau}\right)\right) \qquad (5)$$

and

$$h_2(x) = \frac{1}{\pi}\arcsin\left\{\sin\left[\arccos\left(\cos\left(\frac{2\pi x}{\tau}\right)\right)\right]\right\} \qquad (6)$$

The shapes of $h_1(x)$ and $h_2(x)$ are shown in Fig. 3.

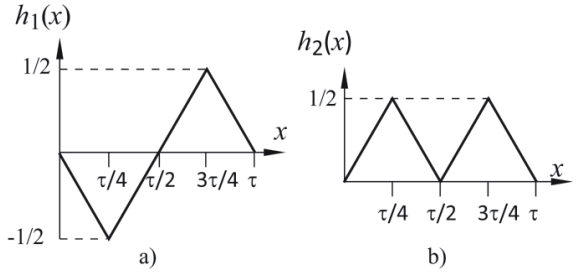

Figure 3. *Auxiliary functions: (a) h1(x), (b) h2(x).*

The derivative of $y(x)$ may be expressed as (Vanegas et al., 2006)

$$y'(x) = \frac{4K_1 y_{\mathrm{a}}}{(1-b)\tau}\left(1 - [b + 2(1-b)h_2(x)]\,\mathrm{e}^{\frac{1-b}{b}(2h_2(x)-1)}\right) \qquad (7)$$

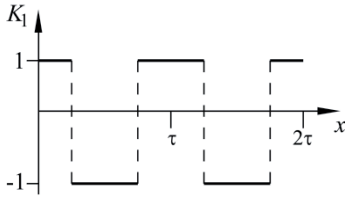

Figure 4. *Auxiliary function K_1.*

where K_1 (Fig. 4) is given by

$$K_1 = \begin{cases} 1, \text{ if int}\left(\dfrac{2x}{\tau} + 0.5\right) \text{ is even} \\ -1, \text{if int}\left(\dfrac{2x}{\tau} + 0.5\right) \text{ is odd} \end{cases} \qquad (8)$$

where the function "int" rounds the argument down to the nearest integer. The peak values of $y'(x)$ are given by

$$y'_{\max} = -y'_{\min} = \frac{4y_{\mathrm{a}}}{(1-b)\tau}\left(1 - b\,\mathrm{e}^{\frac{b-1}{b}}\right) \qquad (9)$$

Examples of $y(x)$ and $y'(x)$ curves are provided in Fig. 5.

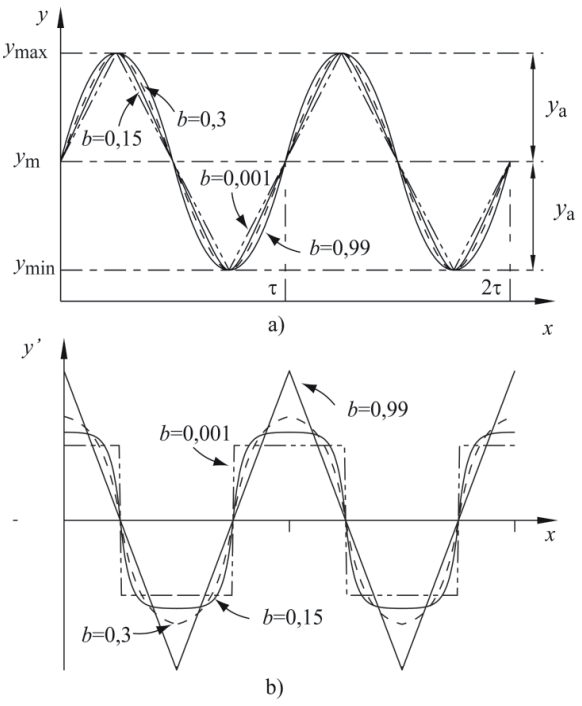

Figure 5. *Examples of the VAP functions for various values of b. (a) y(x); (b) y'(x).*

3. Analysis of a disc cam with radial roller follower

In this section we address the profile of a disc cam with radial roller follower for a given relationship between the cam angular rotation coordinate and the follower displacement coordinate. Fig. 6 shows the cam-follower mechanism after the cam has rotated an angle φ; the cam rotates counterclockwise with angular velocity, ω. The coordinate system oxy is attached to the cam. The follower displacement law, $s(\varphi)$, is given in the design process. Vector $\boldsymbol{R}(\varphi)$ gives the location of point B, which is located on the pitch curve, with respect to the oxy coordinate system. The norm of the vector $\boldsymbol{R}(\varphi)$ is given by:

$$R(\varphi) = R_O + s(\varphi) \tag{10}$$

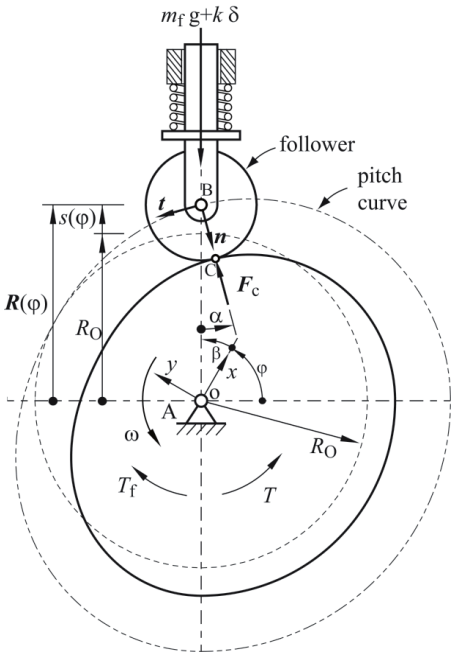

Figure 6. *Cam profile.*

Where R_O is the radius of the prime curve, and $s(\varphi)$ is the follower displacement law. The cam rotation angle, φ, must be differentiated from the polar angle β that determines the position vector of point B with respect the oxy coordinate system. Angles β and φ are related by $\beta(\varphi) = \pi/2 - \varphi$

The components of the position vector of the pitch curve in the oxy coordinate system can be represented by

$$\boldsymbol{R}(\varphi) = \begin{Bmatrix} (R_O + s(\varphi))\cos(\pi/2 - \varphi) \\ (R_O + s(\varphi))\sin(\pi/2 - \varphi) \end{Bmatrix}_{oxy} \tag{11}$$

The polar representation of eq. (11) is

$$\boldsymbol{R}(\varphi) = (R_O + s(\varphi))\, e^{j(\pi/2 - \varphi)} \tag{12}$$

Using this expression, the cam pitch curve can be represented, with respect to the oxy coordinate system, as a function of the cam rotation angle φ as the independent parameter. Normal (***n***) and tangent (***t***) unit vectors of the pitch curve are shown in Fig. 6.

Fig. 6 also shows the contact point, C, between the roller follower and the cam profile. Vector $\boldsymbol{R}_{OC}(\varphi)$ gives the location of point C with respect to the oxy coordinate system; this vector is obtained using:

$$\boldsymbol{R}_{OC}(\varphi) = \boldsymbol{R}(\varphi) + R_f \cdot \boldsymbol{n} \tag{13}$$

where R_f is the radius of the roller follower. The pressure angle, α, can be obtained using the scalar product between the normal vector and the $\boldsymbol{R}(\varphi)$ vector:

$$\alpha = \arccos \frac{\boldsymbol{R}(\varphi) \circ \boldsymbol{n}}{|\boldsymbol{R}(\varphi)|} \tag{14}$$

Where º represents the scalar product.

4. Dynamic analysis of a disc cam with radial roller follower

This section shows the dynamic analysis of the disc cam with radial roller follower under the following considerations: i) the cam angular velocity is constant, ii) the effect of friction on the mechanism is included as a torque applied about the cam shaft, T_f, iii) the cam is balanced, then its center of mass is located on the axis of rotation, iv) the forces on the follower are the contact for ces with the cam, the weight on the follower, m_f g, and the force of the spring, k δ, where m_f is the total follower mass, g is the gravitational constant, k is the spring stiffness, and δ is the spring deformation.

The cam input torque, T, can be obtained using the energy equation on the cam-follower mechanism; it is given by

$$\frac{\mathrm{d}}{\mathrm{d}t}\left(E_{\mathrm{C}}+E_{\mathrm{P}}\right)=P=\sum \boldsymbol{F}_i \circ \boldsymbol{v}_i+\sum T_j \circ \omega_j \qquad (15)$$

where E_{C} and E_{P} are the kinetic and potential energy of the system, respectively; P is the total power of the external forces, $\boldsymbol{F}_i$, and the external torques, T_j. $\mathbf{v}_i$ is the velocity vector of point i where the forces $\boldsymbol{F}_i$ are applied; ω_j is the angular velocity associated with the torque T_j. Eq. (15) gives:

$$\begin{aligned}&\frac{\mathrm{d}}{\mathrm{d}t}\left(\tfrac{1}{2}J_{\mathrm{O}}\,\omega^2+\tfrac{1}{2}m_{\mathrm{f}}s^2+m_{\mathrm{f}}\,\mathrm{g}h+\tfrac{1}{2}k\,\delta^2\right)=\\&m_{\mathrm{f}}\,s\,\ddot{s}+m_{\mathrm{f}}s\,h+k\,\delta\,\dot{s}=T\,\omega-T_{\mathrm{f}}\,\omega\end{aligned} \qquad (16)$$

where $\dot{s}$ is the follower velocity, and h is the height of the follower with respect the reference level of zero potential energy. The derivatives of the follower motion with respect to φ are called pseudo quantities (Flocker, 2007). For example $v(\varphi) = \mathrm{d}s/\mathrm{d}\varphi$ is called pseudo velocity.

$$\dot{s}=\frac{\mathrm{d}}{\mathrm{d}t}s(\varphi)=\frac{\mathrm{d}}{\mathrm{d}\varphi}s(\varphi)\frac{\mathrm{d}\varphi}{\mathrm{d}t}=s'\omega=v(\varphi)\omega$$

Substituting eq. (17) into eq. (16) gives

$$T=\left(m_{\mathrm{f}}\,\ddot{s}+m_{\mathrm{f}}\,\mathrm{g}+k\,\delta\right)s'+T_{\mathrm{f}}$$

The contact forces can be obtained by

$$m_{\mathrm{f}}\,\ddot{s}=F_{\mathrm{C}}\cos\alpha--+m_{\mathrm{f}}\,\mathrm{g}-k\,\delta$$

or

$$F_{\mathrm{C}}=\left(m_{\mathrm{f}}\,\ddot{s}+m_{\mathrm{f}}\,\mathrm{g}+k\,\delta\right)/\cos\alpha$$

5. Illustrative examples

5.1 Kinematic analysis

As case studies, four disc cams with radial roller follower mechanisms are considered; the displacement motions used are: i) a 4-5-6-7 polynomial function, ii) a harmonic function, and ii) two VAP functions with $b = 0.1$ and $b = 0.2$. The radius of the cam prime circle is $R_{\mathrm{O}} = 60$ mm, the radius of the cam base circle is $R_{\mathrm{cb}} = 40$ mm, the radius of the roller follower is $R_{\mathrm{f}} = 20$ mm, the cam angular velocity is taken constant ω = 10 rad/s. The follower rises 30 mm in the first 150º of cam revolution, dwells for an angle of 90º, and then descends in the last 120º of cam rotation. Fig. 7 shows the four displacement motions, Fig. 8 and Fig. 9 show the velocities and the accelerations of the follower for the four proposed displacement motions.

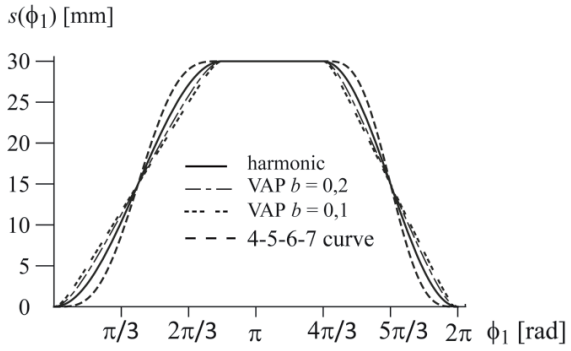

***Figure** 7. Displacement motions.*

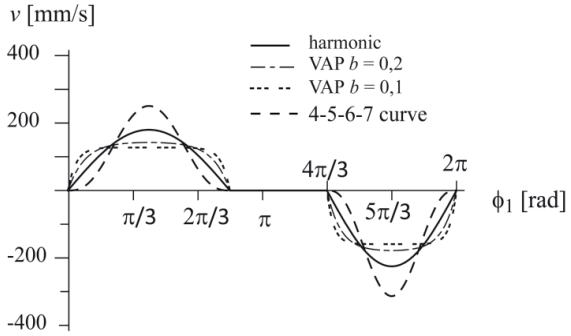

***Figure 8.** Follower velocity.*

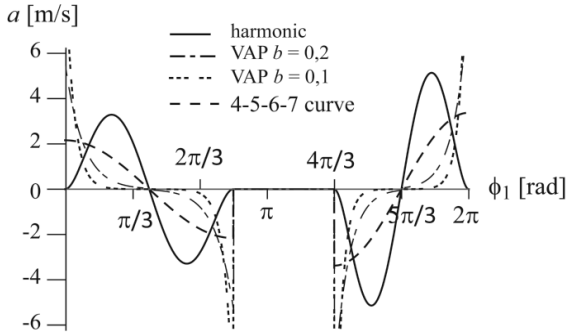

***Figure 9.** Follower acceleration.*

The advantages of using the VAP functions compared with the constant velocity function is that the former avoids the discontinuities of the pseudo velocity obtained with the latter at the beginning and

end of the interval. This characteristic reduces the high inertial forces obtained with the constant velocity the high inertial forces obtained with the constant velocity function. Values of the parameter *b* of the VAP function close to 1.0 make the VAP curve be similar to the curve of the harmonic function.

Fig. 10 shows the curves for the pressure angles of the four cam-follower mechanisms that deliver the proposed displacement laws. The pressure angles for the cam-follower mechanism that delivers the VAP function are lower than the ones obtained with the harmonic function. However, the higher the value of the parameter *b*, the closer the pressure angles of the VAP function to the harmonic function ones.

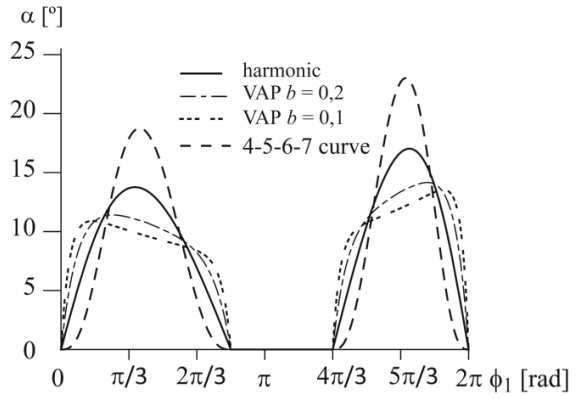

Figure 10. *Pressure angles.*

On the other hand, the lower the value of the parameter *b*, the closer the pressure angles of the VAP function to the constant velocity function ones. However, the pressure angle of the VAP function has lower abrupt changes that the ones of the constant velocity, at the ends of the interval where the dwell meets the curve; the constant velocity has a theoretically infinite acceleration. This acceleration transmits high impact throughout the follower linkage.

5.2 Dynamic analysis

A dynamic analysis is presented in this section. The parameters for this analysis are: weight of the follower m_F g = 1.63 N, the friction torque is constant T_f = 100 N mm, the spring constant k = 100 N/m, the spring deformation is the displacement of the follower.

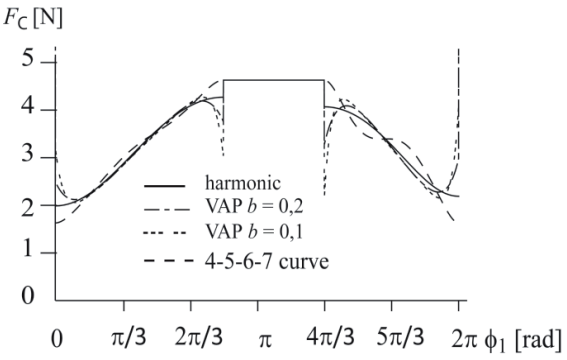

Figure 11. *Contact forces.*

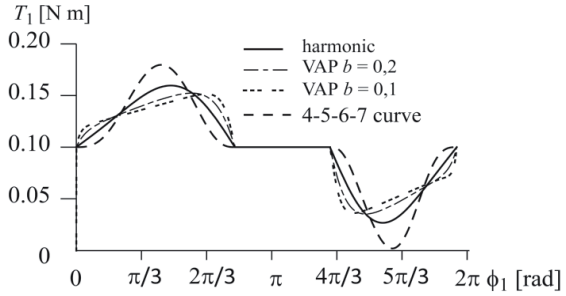

Figure 12. *Input torques.*

Fig. 11 shows the contact forces for the four cam-follower mechanisms that deliver the four specified motions, and Fig. 12 shows their input torques. The use of the cam-follower mechanism obtained with the VAP function smooths the high contact forces produced on the discontinuity points of the displacement motion of the constant velocity. The VAP function will smooth the shape at the beginning and the end of interval and its velocity and acceleration curves are continuous functions.

The maximum input torques of the VAP functions are lower than the one designed with the harmonic function. Again, the use of the cam-follower mechanism designed with the VAP function removes the discontinuity points in the input torque of the mechanism designed with the constant velocity motion. These features avoid impact forces on the mechanism, reduce the stress, and increase the remaining life of the components of the mechanism.

6. Conclusions

This paper analyzed the kinematic and dynamic characteristics of four disc cam – radial roller follower mechanisms. Four displacement laws were analyzed: a 4-5-6-7 polynomial function, a harmonic function, and two VAP functions with two different values of the smoothness parameter. A comparison of the displacements, velocities, and accelerations of the follower; the pressure angles; the contact forces; and the input torques was carried out. The results indicate that the VAP function is a versatile option to design the displacement motions of cam-follower mechanisms; changing a unique smoothness parameter, *b*, enables to modify the displacement law in the design process. According to the results, the pressure angles, and the input torque in the cam-follower mechanism that delivers the VAP function are lower than those of the cam-follower mechanism with harmonic function and the 4-5-6-7 polynomial function. However, the VAP function with small values of the parameter *b* have more abrupt changes of the contact forces that the obtained with the cam-follower mechanism with harmonic function and with 4-5-6-7 polynomial function.

7. References

Catalá, P., De los Santos, M., Veciana, J. & Cardona, S. (2013). Evaluation of the influence of a planned interference fit on the expected fatigue life of a conjugated cam mechanism- a case study. *J. Mech. Des.* 135 (8), 0810021-0810028.

Chan, T., Esedoglu, S. & Nikolova, M. (2005). *Finding the global minimum for binary image restoration*. In Proceedings of the 12th IEEE International Conference on Image Processing (ICIP), Genova, Italy, p. 121-124.

Demeulenaere, B. & De Schutter, J. (2004). Input torque balancing using an inverted cam mechanism. *J. Mech. Des*. 127 (5), 887-900.

Flocker, F. (2007). Controlling the frequency content of inertia forces in dwelling cam-follower systems. *J. Mech. Des.* 129 (5), 546-552.

Flocker, F. (2012). A versatile cam profile for controlling interface force in multiple-dwell cam-follower systems, *J. Mech. Des*. 134 (9), 0945011-0945016.

Flocker, F. (2012b). A Versatile acceleration-based cam profile for single-dwell applications requiring cam-follower clearance during dwell. *J. Mech. Des.*134 (8), 0845051-0845057.

Flores, P. (2013). A computational approach for cam size optimization of disc cam-follower mechanisms with translating roller followers. *J. Mechanisms Robotics* 5 (4), 0410101-0410106.

Gatti, G. & Mundo, D. (2010). On the direct control of follower vibrations in cam-follower mechanisms. *Mech. and Mach. Theory* 45 (1), 23-35.

Hsieh, J. (2010). Design and analysis of cams with three circular-arc profiles. *Mech. and Mach. Theory* 45 (6), 955-965.

Hidalgo, M., Sanmiguel, D. & Burgos, M. (2014). Design of cams with negative radius follower using Bézier curves. *Mech. and Mach. Theory* 82, 87-96.

Jiang, J. & Iwai, Y. (2009) Improving the B-spline method of dynamically-compensated cam design by minimizing or restricting vibrations in high-speed cam-follower systems. *J. Mech. Des.* 131 (4), 0410031-0410038.

Kim, D. (1990). *Dynamics and optimal design of high speed automotive valve trains.* Ph.D. dissertation, North Carolina State University, Raleigh, USA.

Mermelstein, S. & Acar, M. (2003). Optimising cam motion using piecewise polynomials. *Engineering with Computers* 19 (4), 241-251.

Nguyen, V. & Kim, D. (2007). Flexible cam profile synthesis method using smoothing spline curves. *Mech. and Mach. Theory* 42 (7), 825-838.

Peters, D. & Chen, S. (2014). *Design of a cam-actuated robotic leg.* In Proc. of ASME 2014 International Mechanical Engineering Congress and Exposition (IMECE), Montreal, Canada, p. 351-356.

Quintero, H., Cardona, S. & Jordi, L. (2007). The synthesis of an n-lobe noncircular gear using Bézier and B-spline Nonparametric curves in the design of its displacement law. *J. of Mech. Des.* 129 (9), 981-985.

Realmuto, J., Klute, G. & Devasia, S. (2015). Nonlinear passive cam-based springs for powered ankle prostheses, *J. Med. Devices* 9 (1), 01100701-01100710.

Vanegas, L., Abdel-Wahab, M. & Parker, G. (2006). *Design of noncircular gears to minimize shaft accelerations*. In Proceedings of the 8th Biennial ASME Conference on Engineering Systems Design and Analysis, Torino, Italy, p. 421-430.